

N O T I C E

THIS DOCUMENT HAS BEEN REPRODUCED FROM
MICROFICHE. ALTHOUGH IT IS RECOGNIZED THAT
CERTAIN PORTIONS ARE ILLEGIBLE, IT IS BEING RELEASED
IN THE INTEREST OF MAKING AVAILABLE AS MUCH
INFORMATION AS POSSIBLE



Semi-Annual Report to
NASA Langley Research Center
on
FREE-FIELD PROPAGATION OF HIGH INTENSITY NOISE
by

O. H. McDaniel, S. D. Roth, and J. P. Welz

THE NOISE CONTROL LABORATORY

March 18, 1981

(NASA-CR-164032) FREE-FIELD PROPAGATION OF
HIGH INTENSITY NOISE Semiannual Report
(Pennsylvania State Univ.) 30 p
HC A03/MF A01

N81-19873

CSCL 20A

Unclass

G3/71 41637

THE PENNSYLVANIA STATE UNIVERSITY
College of Engineering
Department of Mechanical Engineering
University Park, Pennsylvania

Semi-Annual Report to
NASA Langley Research Center
on
FREE-FIELD PROPAGATION OF HIGH INTENSITY NOISE

NASA Research Grant NAG-I-4

by

Oliver H. McDaniel

and

S. David Roth

and

Joseph P. Welz

THE NOISE CONTROL LABORATORY
THE PENNSYLVANIA STATE UNIVERSITY

March 18, 1981

I. INTRODUCTION¹

The far-field spectrum of a supersonic jet has a distinctly different spectrum than that of a subsonic jet. The spectrum of a supersonic jet diminishes with increasing frequency at a $1/f$ rate (where f is frequency) whereas a subsonic jet spectrum has a slope proportional to $1/f^2$. It was proposed that the difference could be attributed to a nonlinear acoustic rather than aerodynamic effect. Research on high intensity (finite amplitude) acoustic waves has shown that nonlinear distortion effects generally result in a shift of energy to higher frequencies. The higher intensities associated with supersonic jets would therefore indicate that high frequency enhancement of the spectrum should occur, resulting in the differences observed between subsonic and supersonic jets.

Research on high intensity acoustic phenomena has been largely restricted to initially sinusoidal waves. The wave distortion effect in this case for both plane and spherical waves has been extensively treated theoretically and experimentally.

The plane wave theory for initially sinusoidal propagation has been sufficiently verified by experiment and the Bessel-Fubini solution (References 1 and 2) suffices for a large number of plane wave finite amplitude situations. This solution predicts that an initially sinusoidal wave develops into a saw-tooth waveform or acoustic shock wave, thus the shift in energy from the sinusoidal fundamental wave into harmonics of higher frequency.

Substantial portions of sections I and II of this report were presented in our renewal proposal and at the SHOCK NOISE WORKSHOP at NASA Lewis Research Center on December 5, 1980.

Initially sinusoidal spherically diverging high amplitude waves behave in a similar manner; however, higher intensities are required for spherical waves to form shocks since the waves are diminishing in amplitude due to spherical divergence. The theory for the initially sinusoidal spherical case (reference 3) has also been verified experimentally (references 4-5). In both cases, for sufficiently high amplitude, the wave distorts into a stable saw-tooth form with a $1/f$ spectrum which, resembles the spectrum observed for supersonic jet noise.

The propagation of two superimposed initially sinusoidal high intensity waves of two frequencies has also been extensively investigated. The resulting production of a subharmonic at the difference between the two frequencies was predicted theoretically by Westervelt (reference 6) and verified experimentally for propagation in water (reference 7). This phenomena, referred to as the "Parametric Effect", is analogous to intermodulation distortion in electronic circuits and produces sum as well as difference frequencies.

The finite amplitude effects for a single and dual frequency initially sinusoidal waves can be represented in terms of Fourier series for the sound pressure, p , as follows:

SINGLE FREQUENCY

$$p = \sum_{n=1}^{\infty} P_n e^{nj(\omega t - kz)}$$

where P_n = amplitude factor of the n^{th} harmonic

ω = angular frequency of the initially sinusoidal wave

$k = \omega/c$

c = sound velocity

z = spatial coordinate

DUAL FREQUENCY

$$\begin{aligned}
 p = \sum_{n=1}^{\infty} [& P(\omega_1)_n e^{nj(\omega_1 t - k_1 z)} \\
 & + P(\omega_2)_n e^{nj(\omega_2 t - k_2 z)} \\
 & + P(\omega_s)_n e^{nj(\omega_s t - k_s z)} \\
 & + P(\omega_d)_n e^{nj(\omega_d t - k_d z)}]
 \end{aligned}$$

where

$P(\omega_1)_n$ = amplitude factor of the n^{th} harmonic of frequency ω_1

$P(\omega_2)_n$ = amplitude factor of the n^{th} harmonic of frequency ω_2

$$\omega_s = \omega_2 + \omega_1$$

$$\omega_d = \omega_2 - \omega_1$$

$$k_s = (\omega_2 + \omega_1)/c$$

$$k_d = (\omega_2 - \omega_1)/c$$

For the dual frequency case, there is both high and low frequency enhancement of the spectrum. The amplitude factors of the various harmonics for both the single and dual frequency cases are functions of the initial amplitudes and frequencies, the distance from the source, z , the sound velocity c and the medium nonlinearity parameter which for the case of a gas is the ratio of specific heats.

The dual frequency case has been observed in air by Bennett and Blackstock (reference 8) and their results are in good agreement

with the theoretical treatment of Fenlon (reference 9). The power limitations of the sources used by Bennett and Blackstock were such that the difference frequency component was at least 50 dB lower than the primary levels generated at ω_1 and ω_2 . They did not give results for the levels at ω_s .

It is reasonable to assume that for the case of propagation of high intensity broadband random noise that both the progressive wave steepening effect observed for single frequencies and the intermodulation effect of dual frequency propagation are occurring resulting in both low and high frequency spectrum enhancement.

The propagation of high intensity random noise has received considerably less attention than the propagation of initially sinusoidal waves; however, several significant studies have been conducted. Pernet and Payne (reference 10) demonstrated that for a relatively narrow band of high intensity random noise, harmonic bands are generated somewhat analogous to the periodic case. This study was limited to plane waves. In another plane wave study, Pestorius and Blackstock (reference 11) found that for sufficiently high levels of broad band noise that shocks are formed and that there is energy conversion to both the high and low frequency directions; however, the predominant conversion effect is in the high frequencies with a distinct change in the slope of the spectrum.

A study of the propagation of spherically diverging high amplitude random noise has been conducted by Webster and Blackstock

(reference 12). Sound pressure levels of 121 to 145 dB at one meter from the source were generated using a conventional electroacoustic transmitter over a frequency range of 2-10 kHz. Although the acoustic levels were not sufficient to produce acoustic shocks, strong nonlinear behavior was nevertheless observed. Nonlinear high frequency effects were observed over the entire source to receiver propagation path and Webster and Blackstock conclude that the nonlinearly generated high frequency noise never becomes small signal in behavior regardless of distance.

Webster and Blackstock have also investigated the interaction of broad band noise with a sinusoidal signal for the plane wave case (reference 13) and have shown that the broad band noise is drastically altered in both spectrum shape and level by the presence of the periodic wave. This effect has, however, not been investigated for the case of spherical propagation. If this strong interaction does occur for the spherical case it would imply that the characteristics of noise radiation from the exhaust of a jet engine could be altered by the presence of periodic waves originating from the compressor, turbine or oscillations due to instabilities.

In this current research program the work of Webster and Blackstock on free-field propagation of finite amplitude noise (reference 12) is being extended to considerably high source intensity levels more representative of an actual supersonic jet.

A 10,000 acoustic watt source has been installed in an anechoic chamber. The levels generated by the source are sufficient such that acoustic shocks are readily observed. In addition, dual frequency excitation of the source has produced a strong parametric effect with a difference frequency comparable in level to the primary frequencies.

II. STATUS OF EXPERIMENTAL PROGRAM

A Ling Model EPT-200 high intensity acoustic source has been installed in the Noise Control Laboratory anechoic chamber. The associated operating system consisting of a 3.5 kw power amplifier, field supply and cooling system, and spectrum shaping equipment has been installed in the Laboratory Control room. An existing compressed air control system has been modified to provide the necessary air flow and pressure requirements of the source. The source is electrically modulated and can therefore generate both broad band and periodic waveforms. An exponential horn is coupled to the source to provide efficient acoustic power transfer to the free-field environment of the anechoic chamber. Photographs of the transducer installation, operating system, air education system and analysis equipment are shown in figures 1 and 4. The acoustic field is measured with a 1/4" B & K microphone mounted on a linear traversing mechanism. The results to date have been obtained by manually positioning the microphone at various distances from the source. For future experiments a radial traversing mechanism will also be installed and computer controlled stepping motors will be used for both linear and radial positioning of the microphone. In addition, controls for the air supply system are currently being computerized.

The data analysis system consists of a Nicolet Model 660A dual channel Fast Fourier Transform Analyzer with a dedicated dual disk storage unit. The results are plotted with Tektronix digital plotter. The analyzer is interfaced with a Commodore 32K microcomputer which also has dual disc storage.

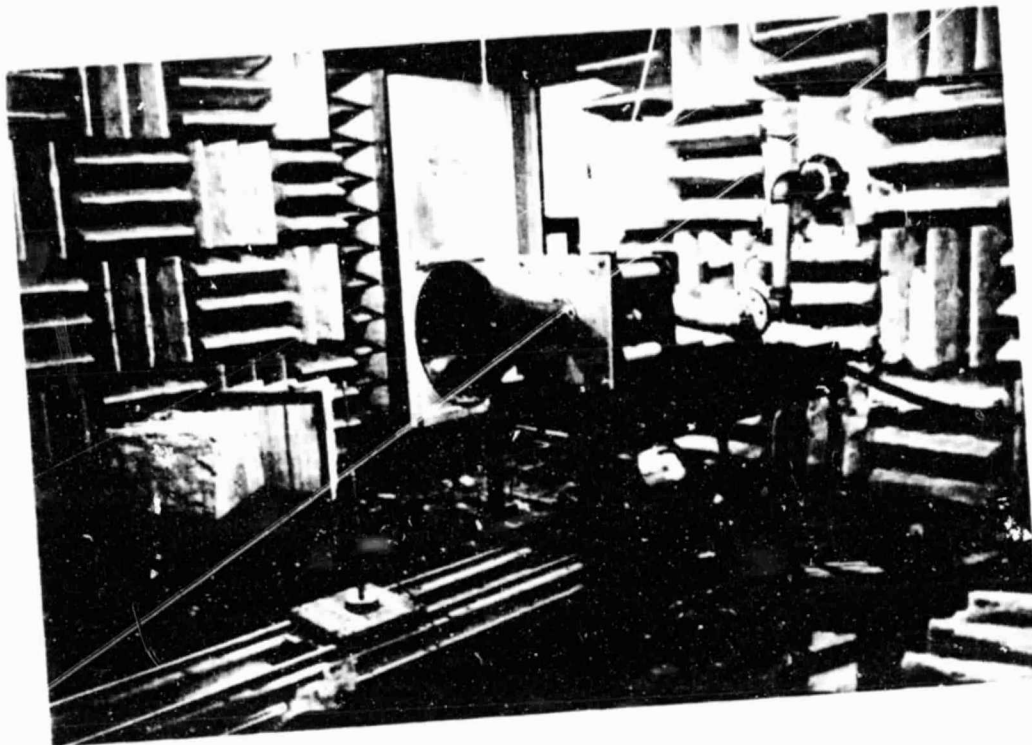


FIGURE 1. Source Installed in Chamber

ORIGINAL PAGE IS
OF POOR QUALITY

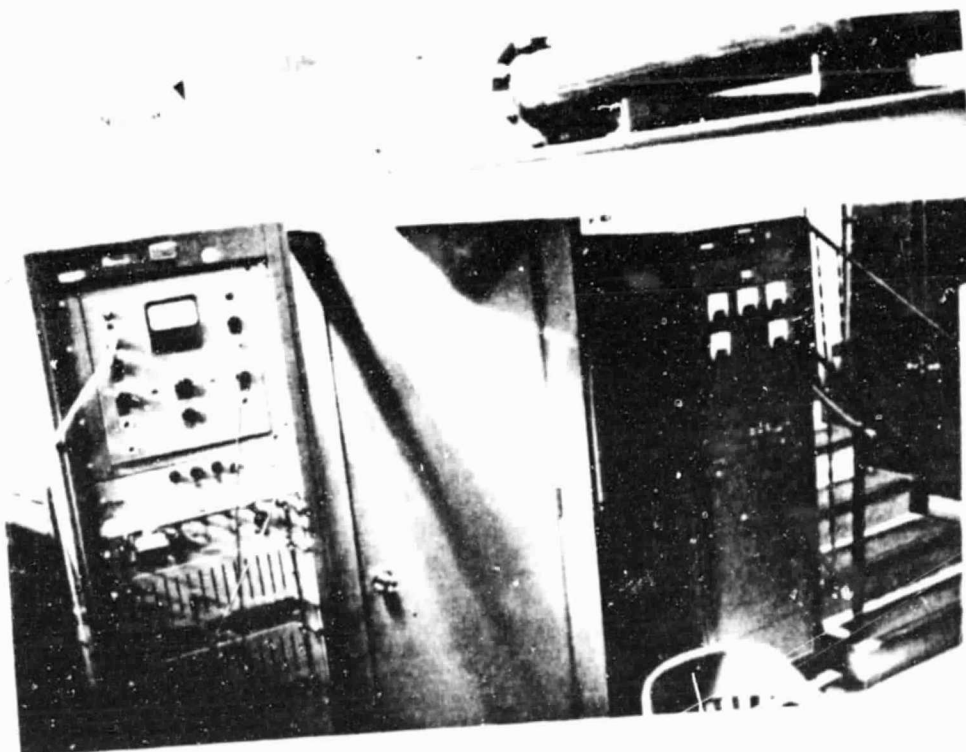


FIGURE 2. Operating System

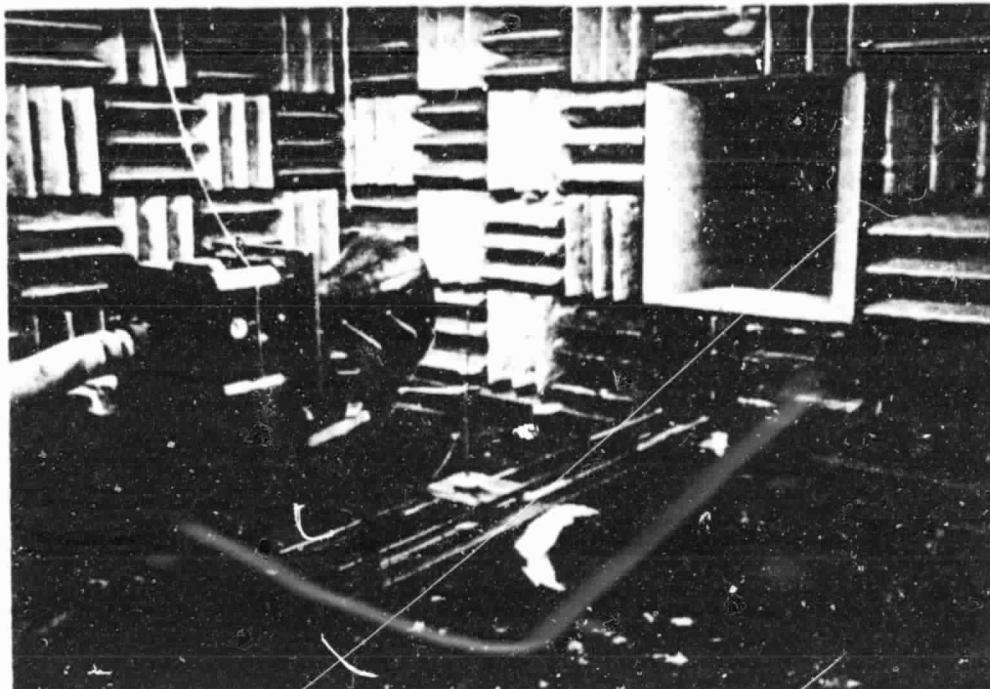


FIGURE 3. Air Education System

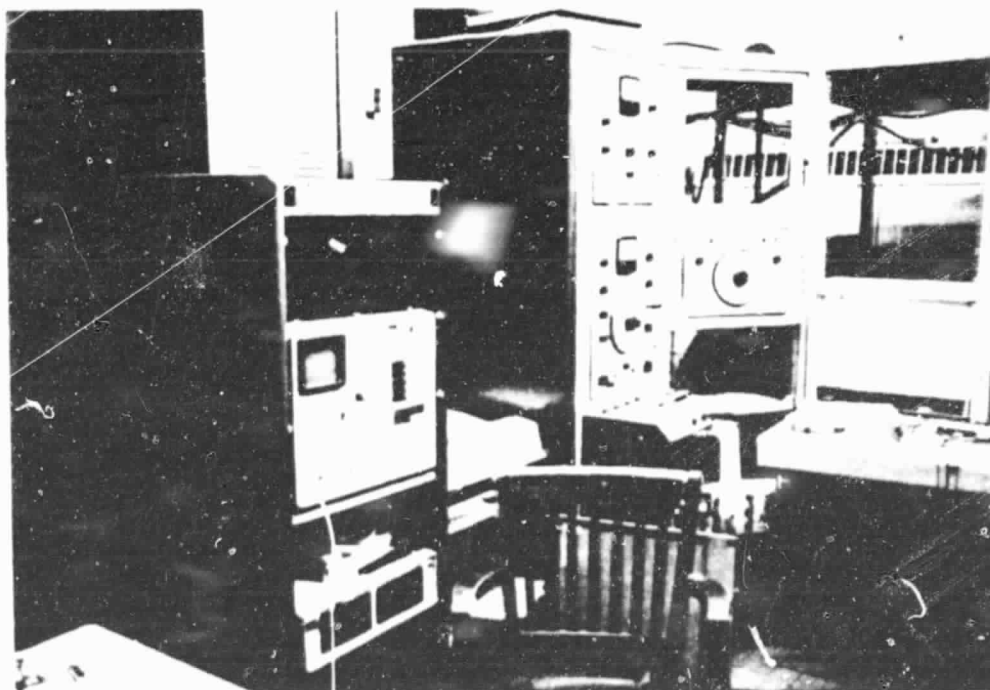


FIGURE 4. FT Analysis Instrumentation

Preliminary results have been obtained for source excitation with band limited noise, sine waves, and dual sine waves. Typical results for band limited noise are shown in figures 5 through 11. The spectrum shaper was adjusted for equal output at the 630, 800, 1000, and 1250 Hz one-third octave bands with all other bands off. The waveform of the electrical input to the power amplifier is shown in figure 5. The total time span of this record and of figures 7, 9, and 11 is .008 seconds. The spectrum of this signal is shown in figure 6. The vertical scales on all spectra shown is 10 dB per division. The acoustic output at 3-1/2 feet from the source is shown in figures 7 and 8. The sound pressure level at this position is 158 dB. The wave steepening effect is quite evident and the enhancement of high frequencies in the spectrum is present. The acoustic output at 7 feet is shown in figures 9 and 10. The waveform is steeper than at 3-1/2 feet and the high frequency content continues to increase with a change in slope of the spectrum. Continued steepening of the waveform is illustrated in figure 11 for a 10 foot microphone position.

Spectra for a single 1/3 octave band of noise are shown in figures 12 through 15. A logarithmic frequency scale is used in this case. The electrical input spectrum is shown in figure 12. The spectra at .5 feet and 7.5 feet are shown in figures 13 and 14 and the waveform at 7.5 feet is shown in figure 15. The spectrum shift and steep waveform are well illustrated

The waveform and spectrum for a 1 kHz sine wave input are shown in figures 16 and 17 measured at 4 feet with a sound pressure level

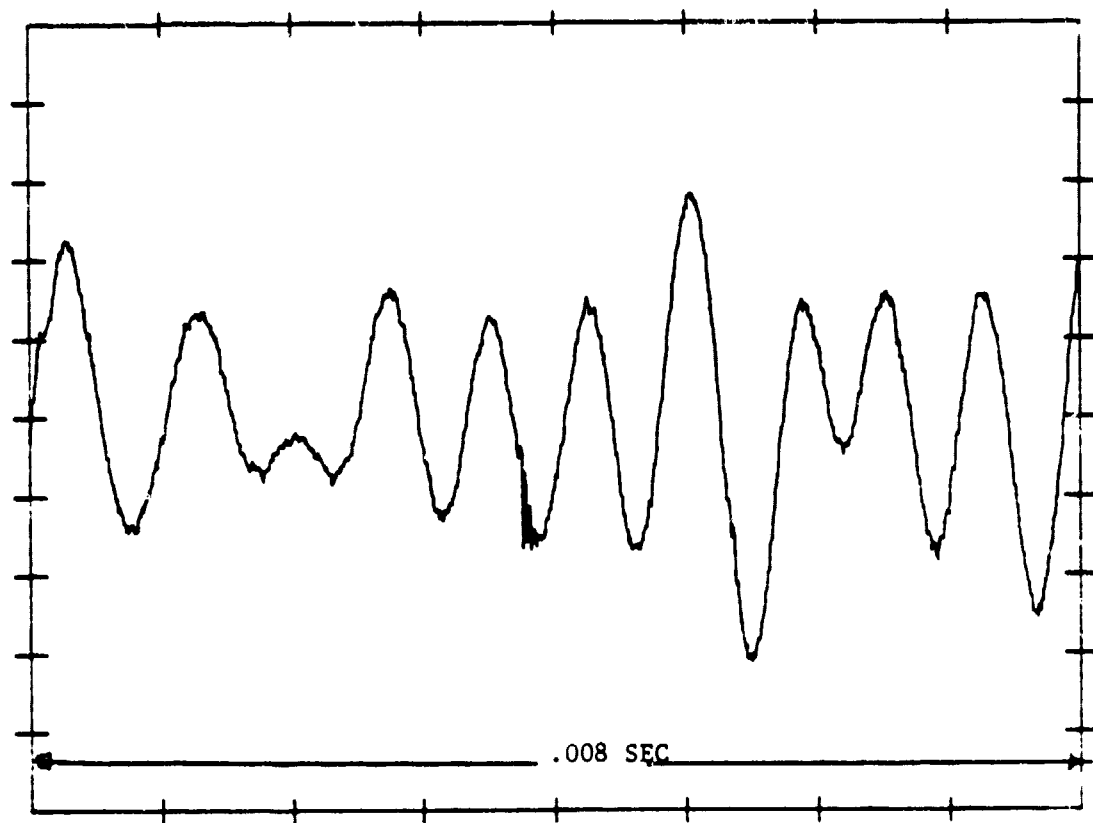


FIGURE 5. Waveform of Electrical Input, Band Limited Noise

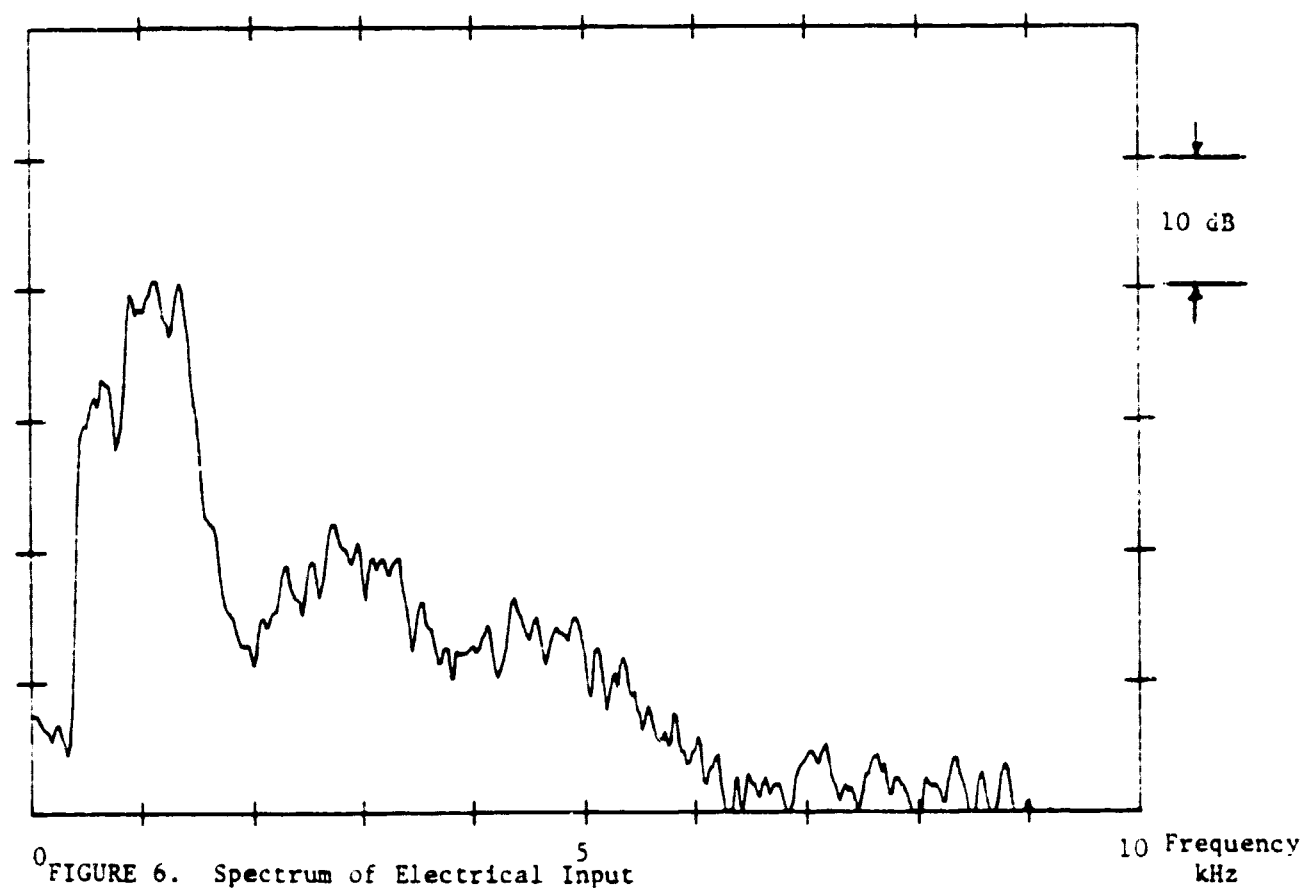


FIGURE 6. Spectrum of Electrical Input

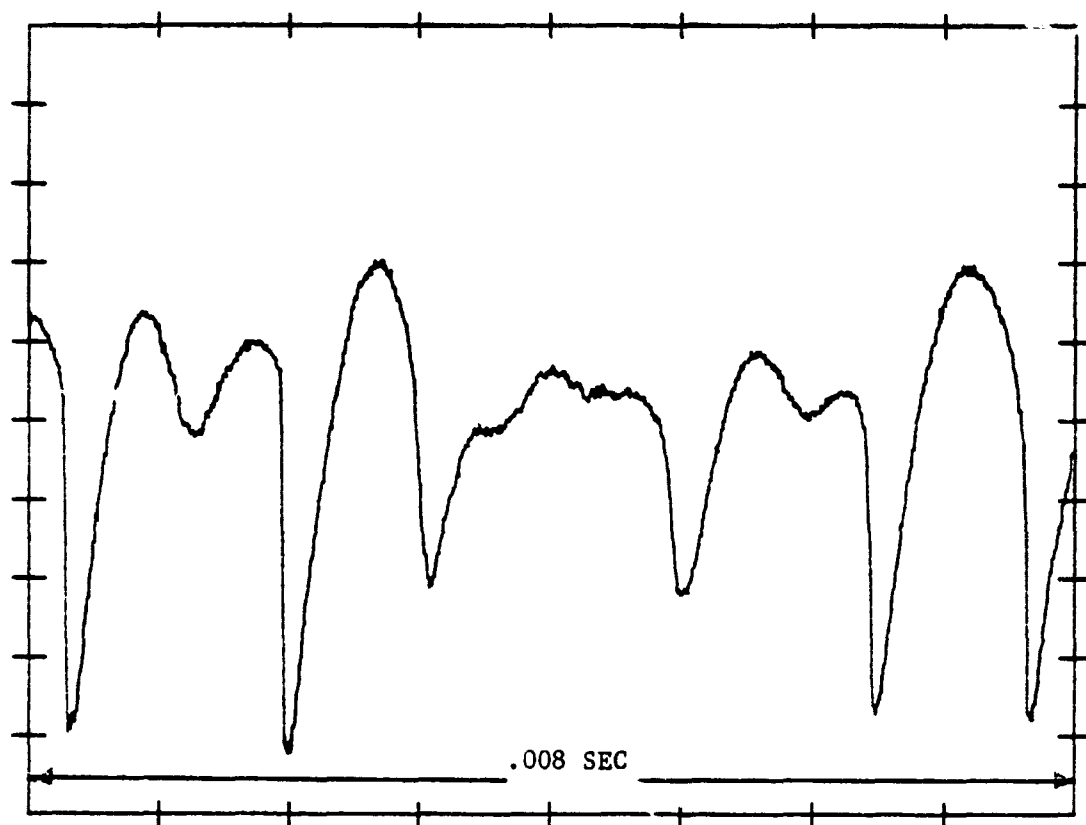


FIGURE 7. Waveform of Acoustic Output at 3-1/2 feet from Source

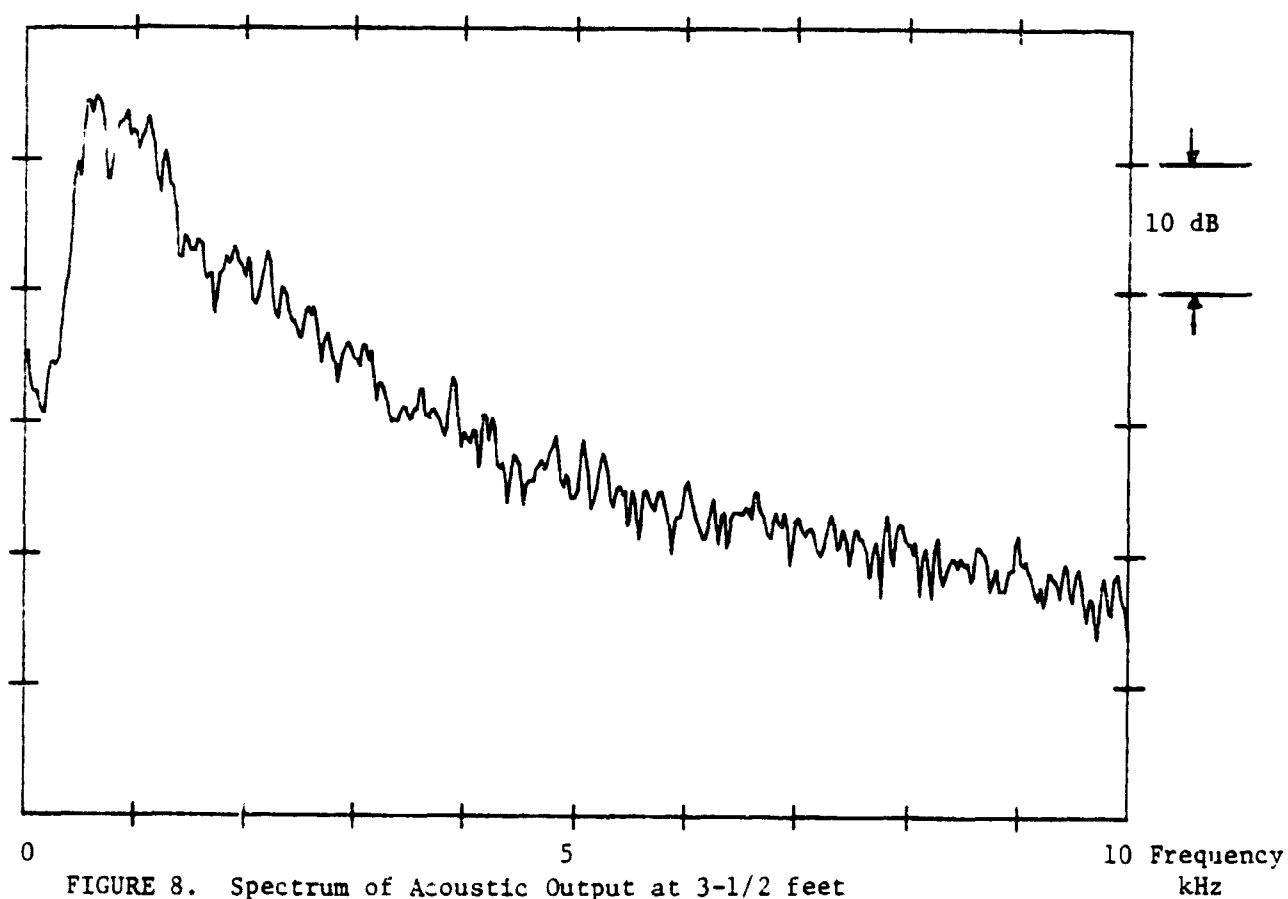


FIGURE 8. Spectrum of Acoustic Output at 3-1/2 feet

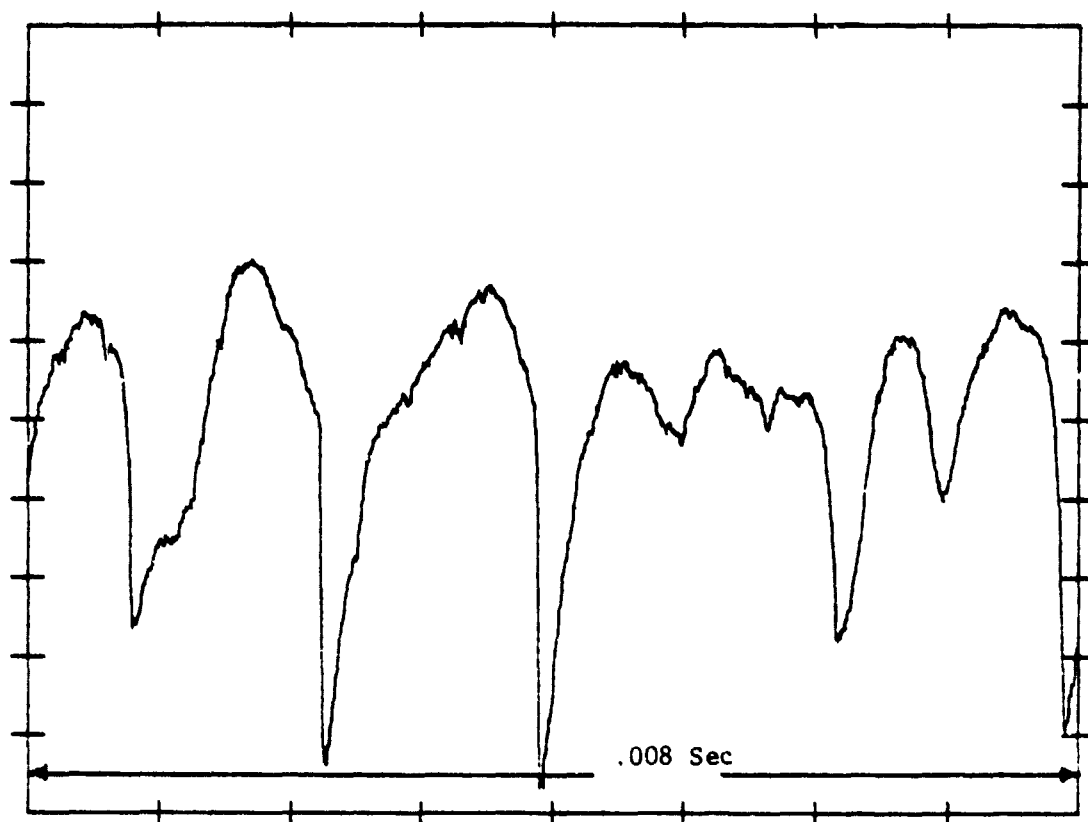


FIGURE 9. Waveform of Acoustic Output at 7 feet from Source.

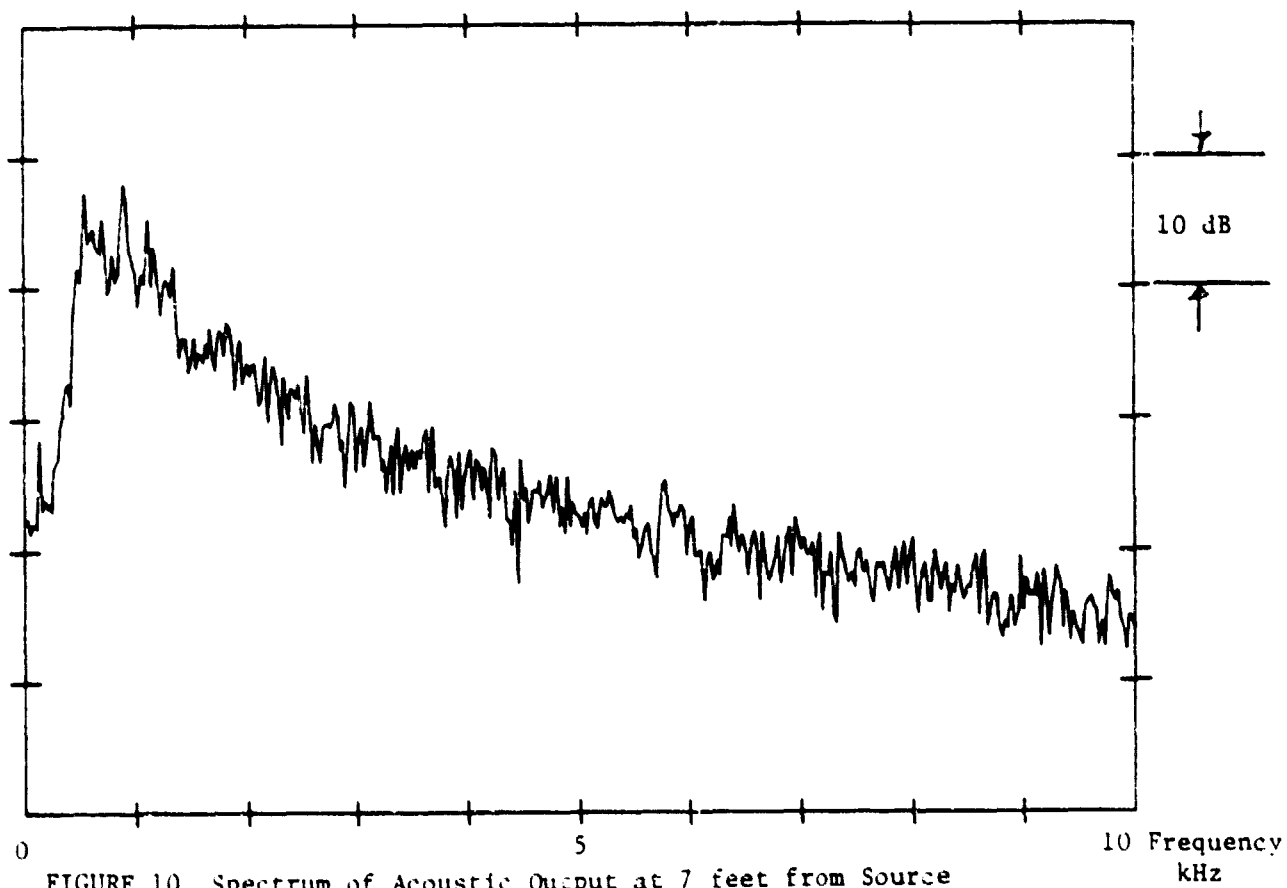


FIGURE 10. Spectrum of Acoustic Output at 7 feet from Source

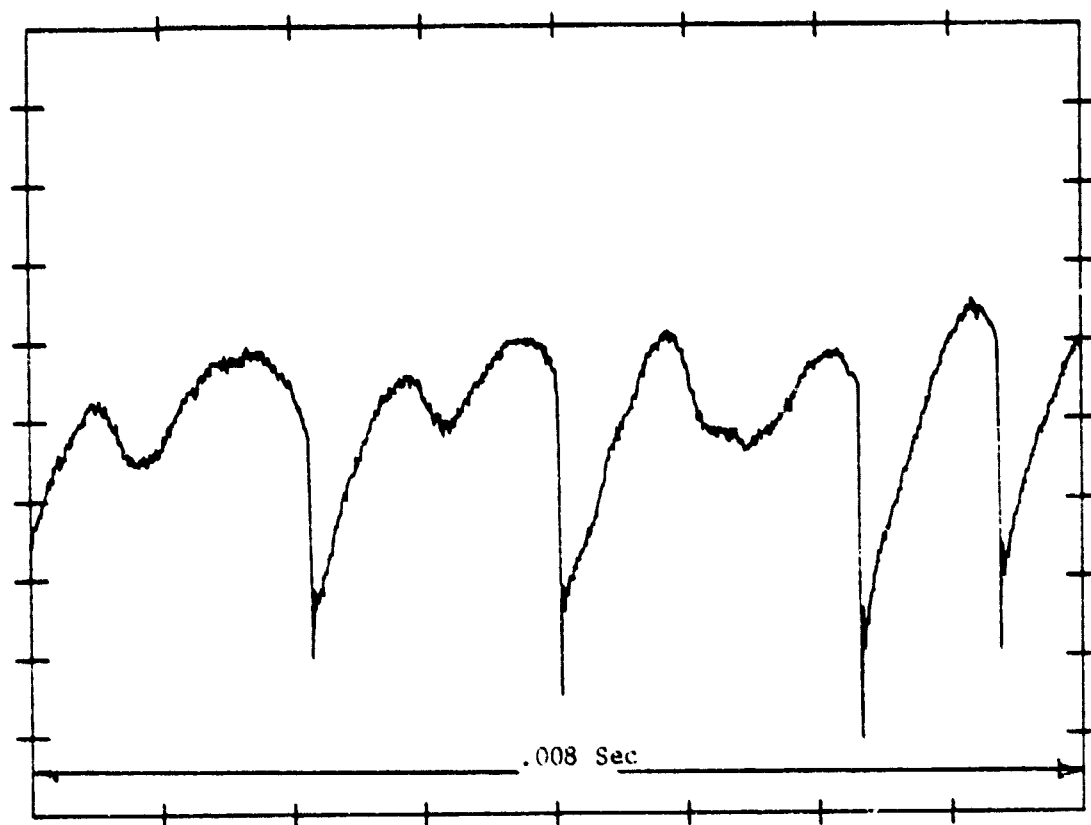


FIGURE 11. Waveform of Acoustic Output at 10 feet from Source, 15° off-axis

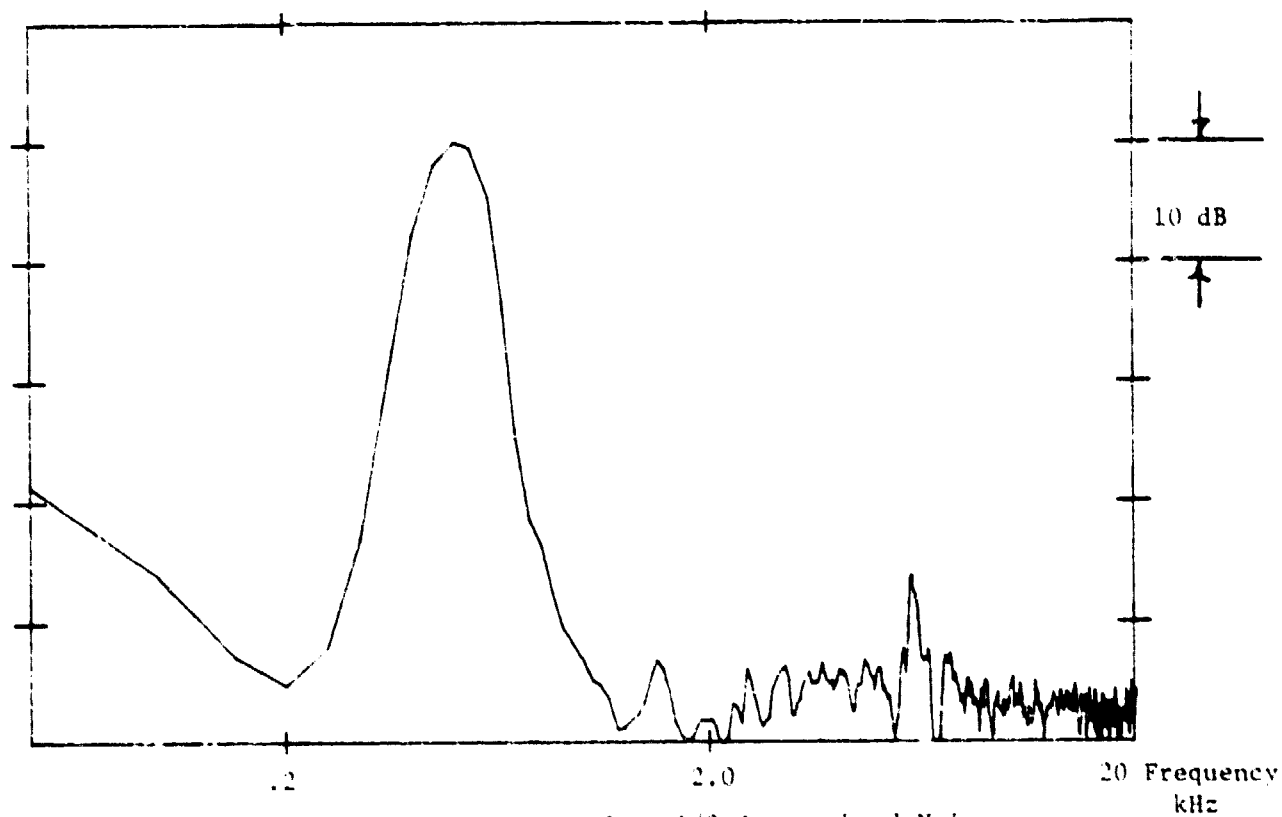


FIGURE 12. Electrical Input Spectrum from 1/3 Octave-band Noise

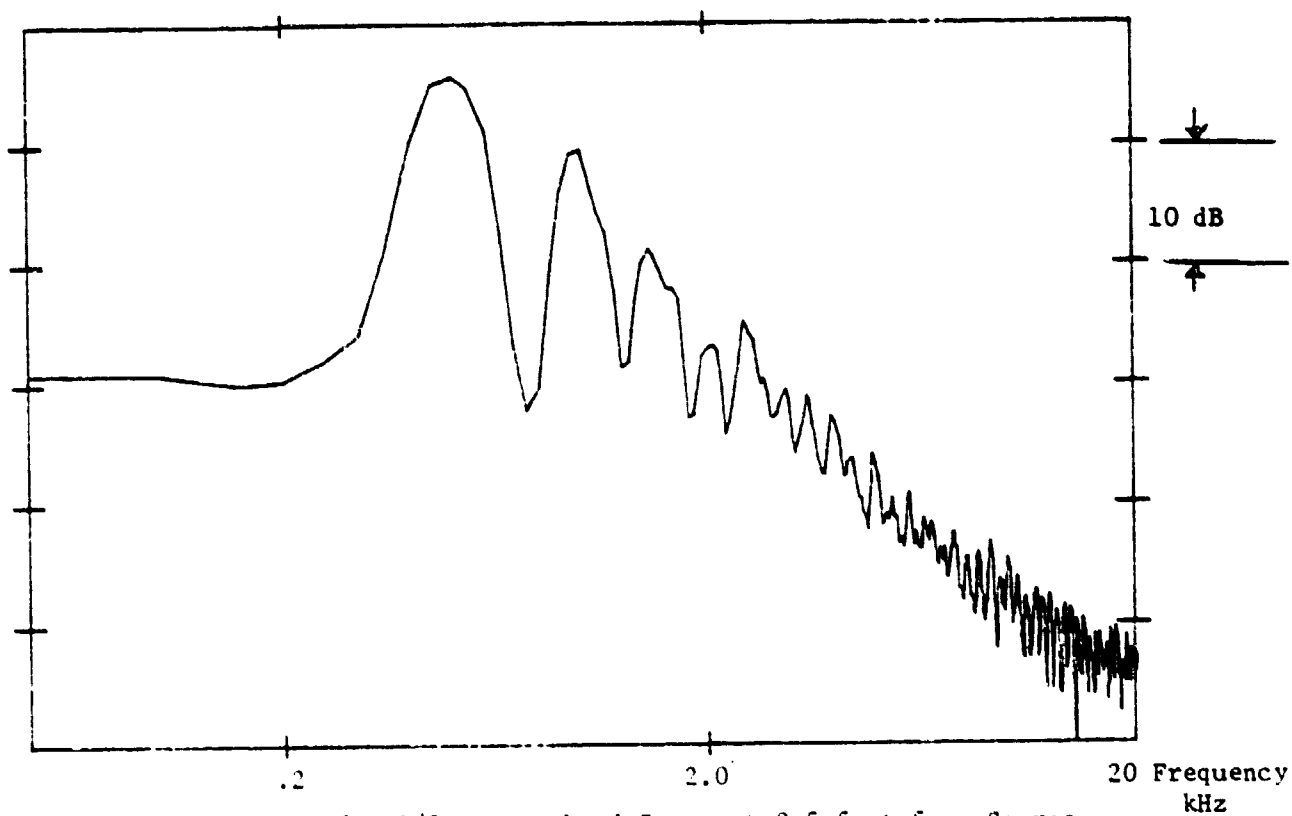


FIGURE 13. Spectrum for 1/3 Octave-band Input at 0.5 feet from Source

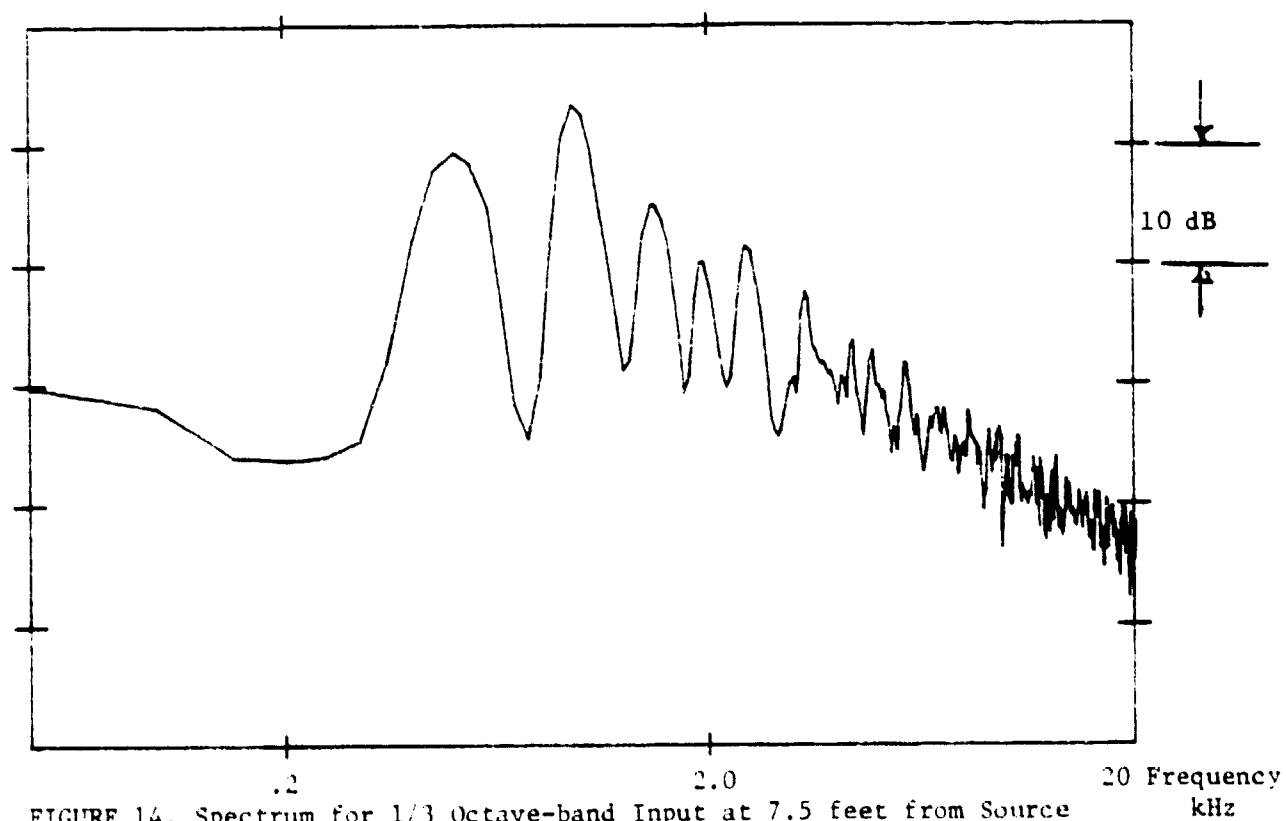


FIGURE 14. Spectrum for 1/3 Octave-band Input at 7.5 feet from Source

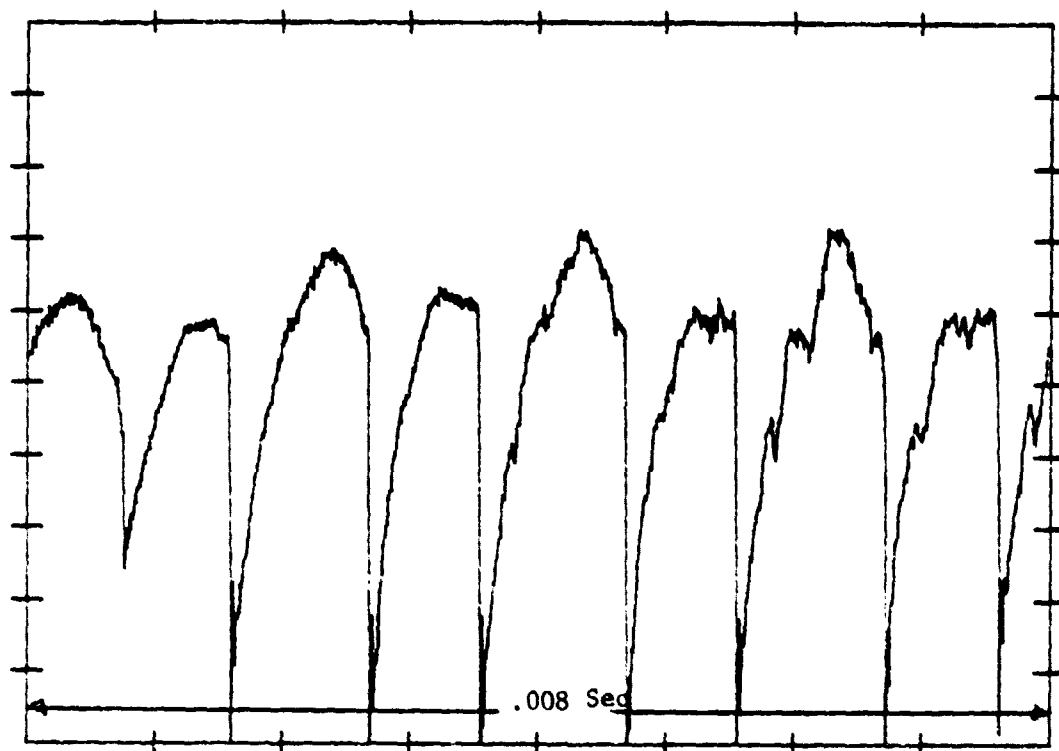


FIGURE 15. Waveform of 1/3 Octave-band Noise at 7-1/2 feet.

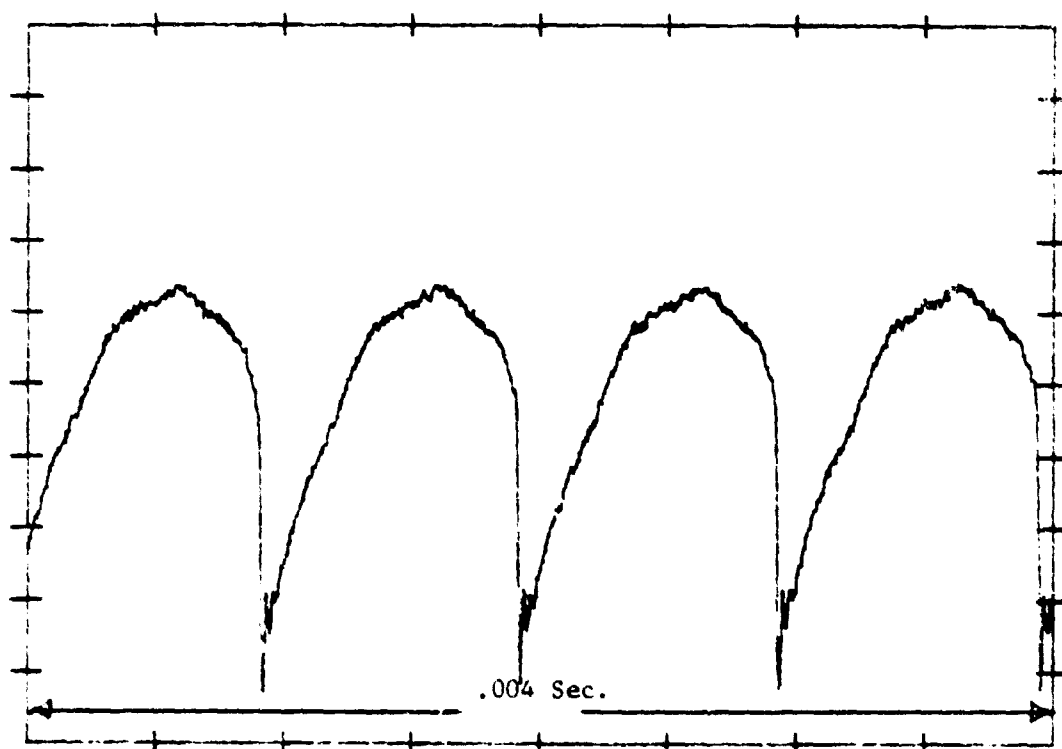


FIGURE 16. Waveform for 1 kHz Sine Wave Input Measured at 4 feet from Source

of 158 dB.

Dual frequency excitation is shown in figures 18 and 19 for input frequencies of 800 and 1000 Hz. In this case the difference frequency component generated is higher than the components at 800 and 1000 Hz.

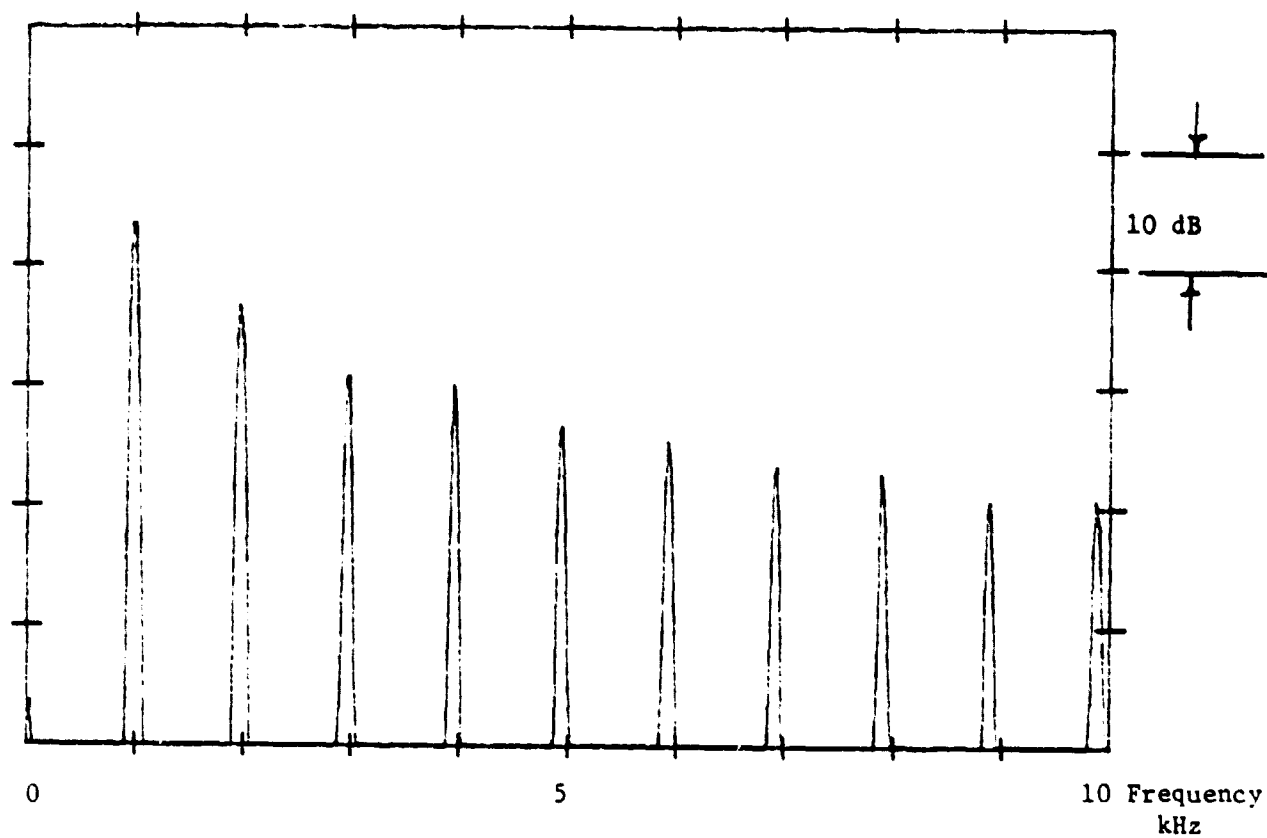


FIGURE 17. Spectrum for 1 kHz Sine Wave Input Measured at 4 feet from source.

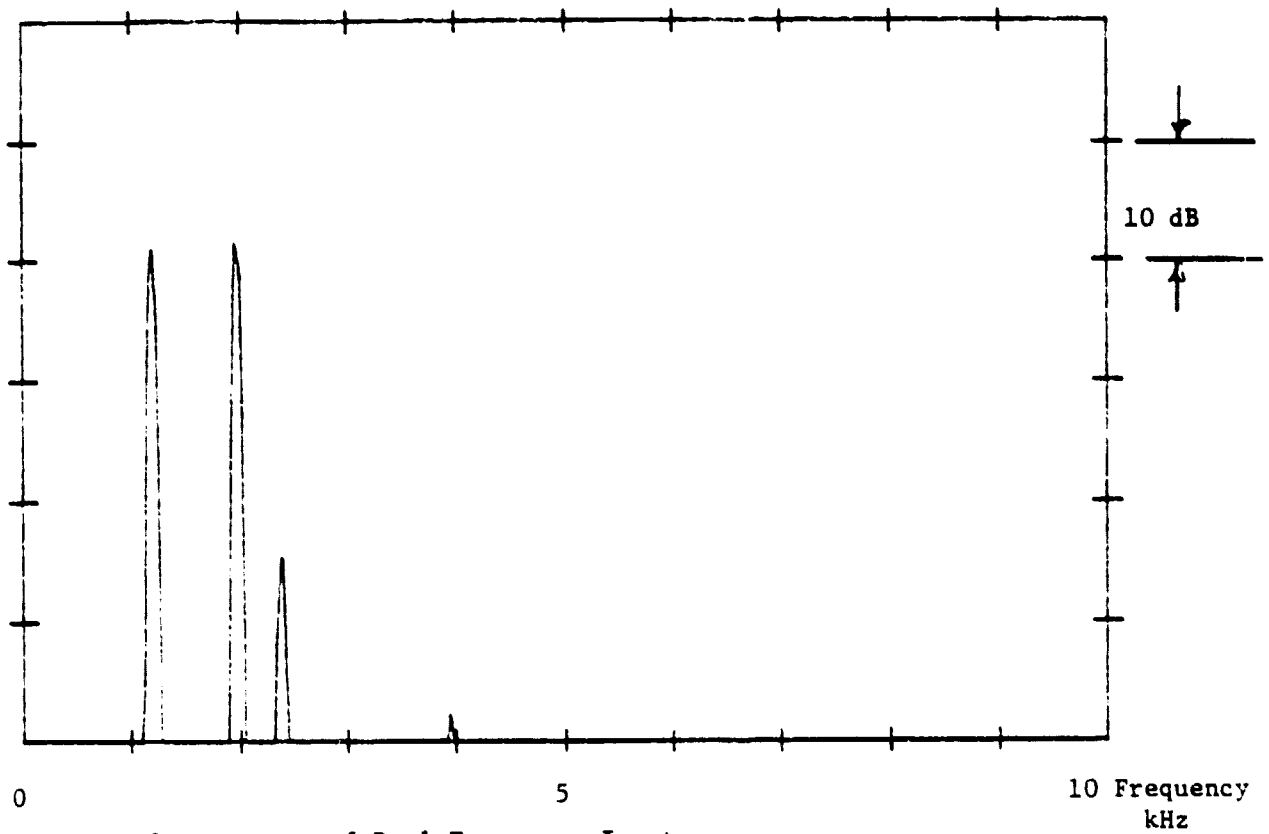


FIGURE 18. Spectrum of Dual Frequency Input

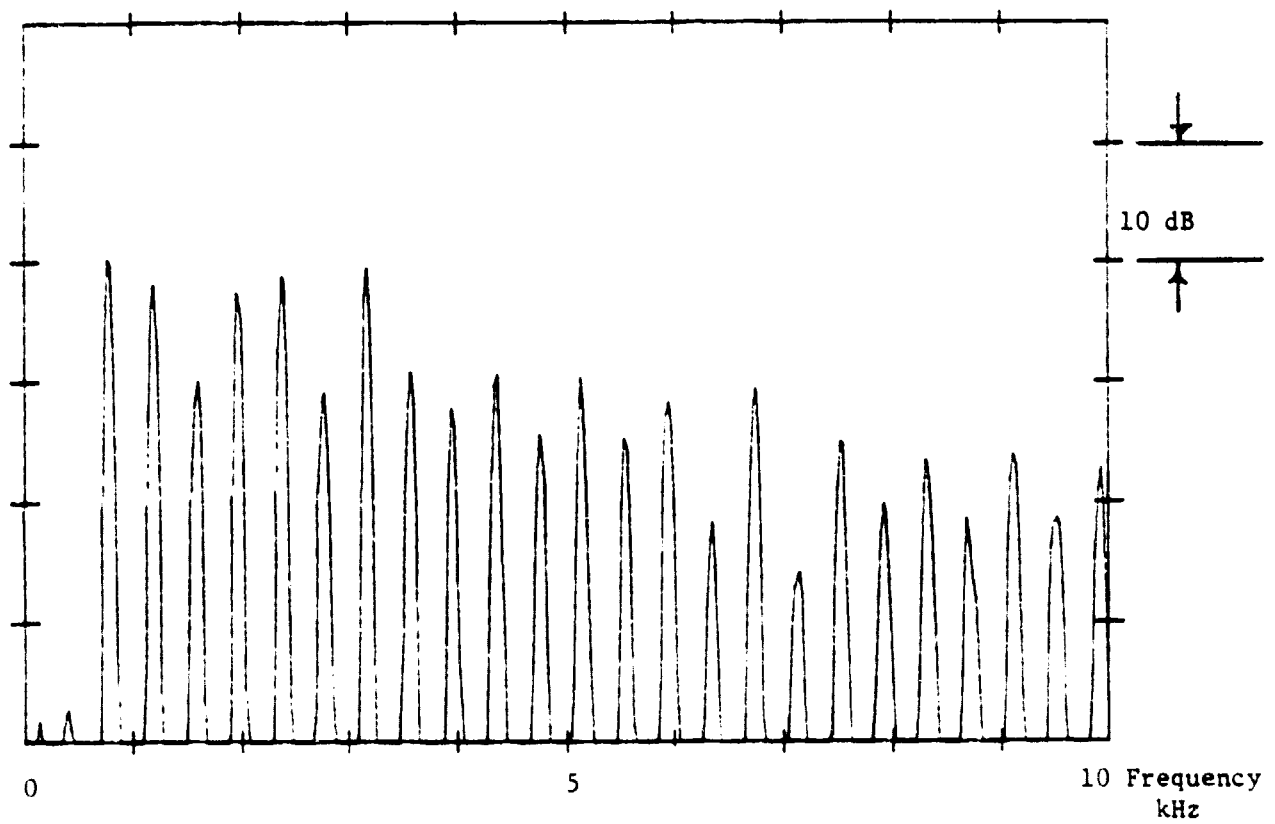


FIGURE 19. Acoustic Spectrum for Dual Frequency Input

III. STATUS OF THEORETICAL INVESTIGATION

This study is largely based on an application of Burger's equation developed by McKendree and Fenton (reference 13). Burger's equation is a second order form of the wave equation. It describes suitably the propagation of sound in a non-linear medium.

Burger's equation may be written as

$$\frac{\partial p}{\partial \sigma} - p \frac{\partial p}{\partial \tau} - \frac{1}{\Gamma} \frac{\partial^2 p}{\partial \tau^2} = 0 \quad (1)$$

where for spherical waves

$$p = \frac{r}{r_0} \frac{p'}{p_{\max}}$$

$$\sigma = \beta \epsilon k r_0 \ln \frac{r}{r_0}$$

$$\tau = \omega \left(\tau - \frac{r}{c_0} \right)$$

$$\Gamma = \frac{\beta \epsilon k}{\alpha_w}$$

and

$$r_0 \equiv \text{Rayleigh distance} = \frac{ka^2}{2} \text{ for a circular piston with radius } a$$

$$\beta \equiv \frac{\gamma+1}{2} \quad \gamma = \frac{C_p}{C_v} = 1.4 \text{ in air}$$

$$\epsilon \equiv \text{peak Mach number}$$

$$\alpha_w \equiv \text{viscous absorption/wavelength}$$

$$p' \equiv \text{peak pressure}$$

$$r \equiv \text{radial distance}$$

$$c_0 \equiv \text{phase velocity}$$

The term $k = \frac{\omega}{c_0}$ has presented a problem. In the development of solutions to Burger's equation, this term has been considered arbitrary. Indeed, it is arbitrary for the plane wave solution. However, in the spherical wave solution it can play a very important role. If a shock will form, it will form at $\sigma = 1$. To minimize the distance r this corresponds to k must be defined by

$$k^2 = \frac{4}{\beta \epsilon \alpha^2}$$

for a circular piston source. Due to spherical spreading, however, a shock may never form.

Returning now to equation (1). Assuming that terms can be separated we may apply

$$\frac{\partial p}{\partial \sigma} - p \frac{\partial p}{\partial \tau} = 0 \quad (2)$$

over a small increment $\Delta\sigma$ and then apply

$$\frac{\partial p}{\partial \sigma} - \frac{1}{\tau} \frac{\partial^2 p}{\partial \tau^2} = 0 \quad (3)$$

over the same interval $\Delta\sigma$.

Equation (2) is simply the inviscid case of Burger's equation and may be solved using a finite difference solution. It then becomes after slight manipulation

$$p(\sigma, \tau) = p(0, \tau) + \sigma p(\sigma, \tau) \frac{\partial p}{\partial \tau} \quad (4)$$

where σ is now used in place of $\Delta\sigma$, a small increment.

Since $\sigma p(\sigma, \tau)$ is small, and p is a well behaved function in σ the terms in equation (4) may be approximated by the first two terms of a

Taylor's series. Therefore,

$$p(\sigma, \tau) = p(0, \tau) + \sigma p(0, \tau) \frac{\partial p}{\partial \tau}(0, \tau) \quad (5)$$

Equation (5) is the basis of the present computer model. Viscous losses have not yet been included but may be using equation (3) over each increment of σ in equation (5).

The model was first tested using an initially sinusoidal input waveform as shown in figure 20. Figures 21-23 show the waveform steepening and shock formation. The next step in this theoretical study will be to use actual experimentally measured random initial waveforms and compare the waveform and spectrum alteration predicted by the theory with the experimental data.

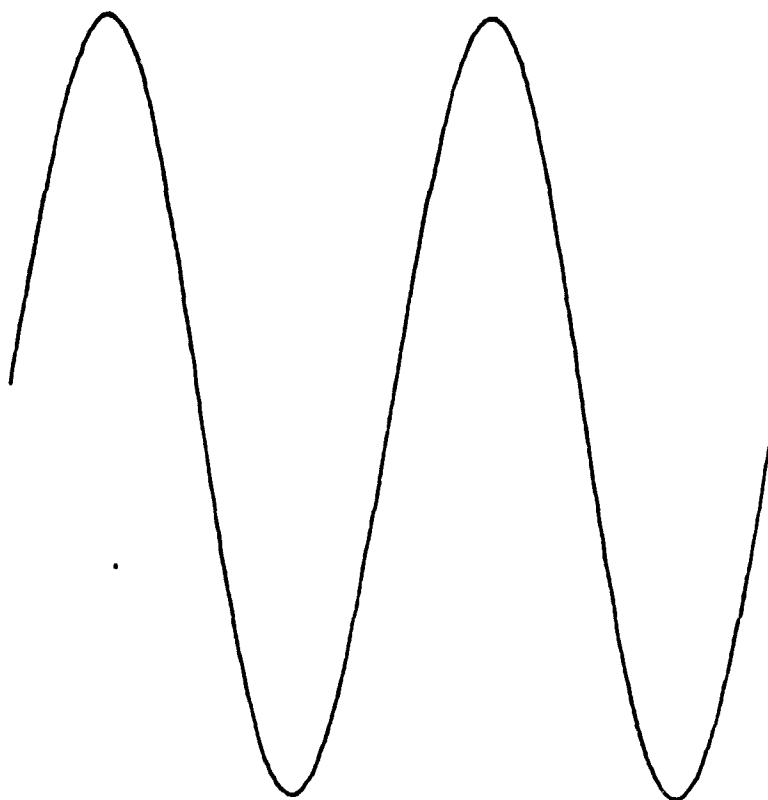


FIGURE 20. Input Waveform

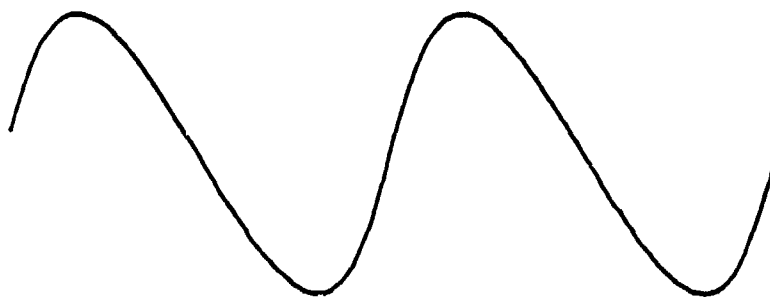


FIGURE 21. Waveform at $z = .025$

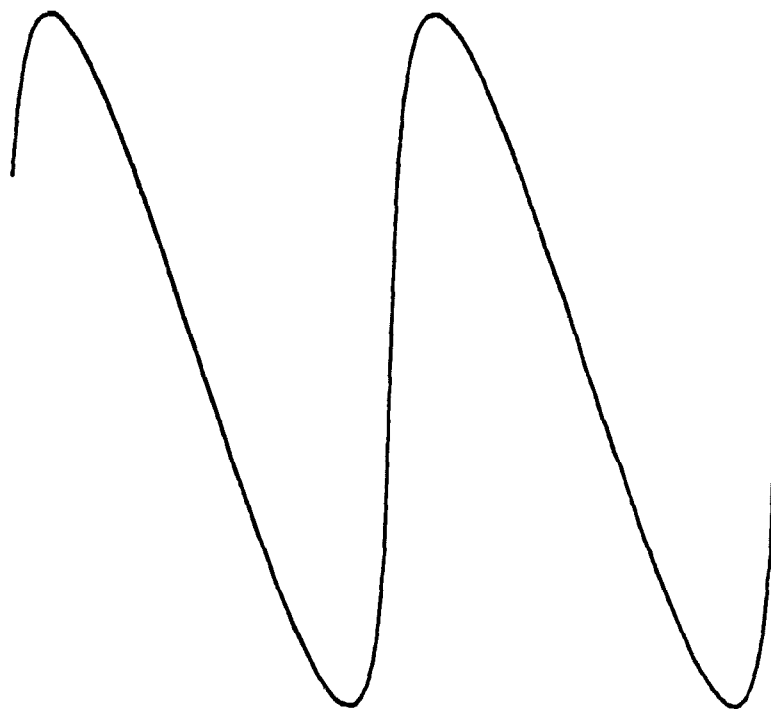


FIGURE 22. Waveform at $z = 0.1$
Amplitude Scale Increased $\times 10$

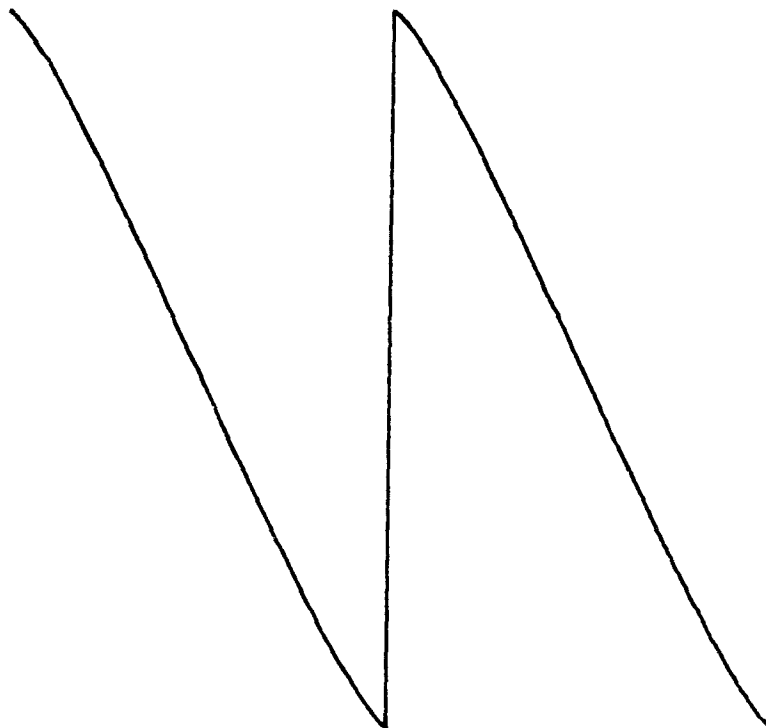


FIGURE 23. Waveform at $Z = 1.0$
Amplitude Scale $\times 100$

IV. REFERENCES

1. E. Fubini-Ghiron, "Anomalie nella Propagazione di Onda Acustiche di Grande Amprezza," Alta Frequenza, 4, pp. 530-581, 1935.
2. D.T. Blackstock, "Propagation of Plane Sound Waves of Finite Amplitude in Nondissipative Fluids," J. Acoust. Soc. Am., 34, pp. 9-30, 1962.
3. K. A. Naugol'nykh, "Propagation of Spherical Sound Waves of Finite Amplitude in a Viscous Heat-Conducting Medium," Soviet Physics-Acoustics 5, pp. 79-84, 1959.
4. E. V. Romanenko, "Experimental Investigation of the Propagation of Finite Amplitude Spherical Waves," Soviet Physics-Acoustics 5, pp. 100-104, 1959.
5. O.H. McDaniel, "Propagation of Sound at Moderate and High Intensities in Absorbent and Hard-Walled Cylindrical Ducts," Doctor of Philosophy, The Pennsylvania State University, March 1975 (Chapter 3).
6. P.J. Westervelt, "Parametric Acoustic Array," J. Acoust. Soc. Am. 35, pp. 535-537 (1963).
7. J.L.S. Bellin and R.T. Beyer, "Experimental Investigation of an End-Fire Array," J. Acoust. Soc. Am. 34, pp. 1051-1054 (1962)
8. M. B. Bennett and D.T. Blackstock "Parametric Array in Air," J. Acoust. Soc. Am. 57, pp. 562-568 (1975).
9. F.H. Fenlon, "On the Performance of a Dual Frequency Parametric Source via Matched Asymptotic Solutions of Burgers' Equation," J. Acoust. Soc. Am. 55, pp. 35-46 (1974)
10. D. F. Pernet and R.C. Payne, "Propagation of Finite-Amplitude Noise in Tubes," National Physical Laboratory, NPL Aero Report Ac. 48, March 1971.
11. F.M. Pestorius and D.T. Blackstock, "Propagation of Finite Amplitude Noise," from Finite-Amplitude Wave Effects in Fluids, Proceedings of the 1973 Symposium-Copenhagen, Edited by L. Bjørnø, IPC Science and Technology Press, 1974.
12. D.A. Webster and D.T. Blackstock, "Experimental Investigation of Outdoor Propagation of Finite-Amplitude Noise," NASA Contractor Report CR-2992.
13. D.A. Webster and D.T. Blackstock, "Collinear Interaction of Noise with a Finite-Amplitude Tone," J. Acoust. Soc. Am. 63, pp. 687-693 (1978).

IV. REFERENCES

14. F. McKendree, "A Numerical Solution to the Second Order Nonlinear Wave Equation in One and Three Dimensions," Ph.D. Thesis in Acoustics, The Pennsylvania State University, 1980. Advisor: F.H. Fenlon